University of Amsterdam

Research Master's Program Brain and Cognitive Sciences, Second Internship Report

Striatum connectivity in gambling disorder

Matheus Boger
Student Number: 14163799

supervised and examined by
Dr. Ruth J. van Holst
Amsterdam UMC

assesed by
Marieke van der Pluijm
Amsterdam UMC

August 2, 2024

Abstract

Gambling disorder (GD) is characterized by persistent gambling to the detriment of an individual's quality of life. It is also highly associated with impulsivity, since many people with GD show a deficit in the inhibition of impulses. fMRI studies have shown altered activation patterns in different brain areas in people with GD when compared to healthy controls (HCs). However, connectivity studies that disentangle the influences of one area onto the other over time are still lacking. Of special interest is the striatum, since it is a core node in the reward system, which is known to play a key role in the disorder. The striatum is functionally subdivided in three areas, motivational (ventral), cognitive and motor (both dorsal), and it is thought that the impulsivity observed in GD could be due to a higher influence of the ventral striatum onto the dorsal striatum, which would fail at inhibiting strong motivational impulses, such as the urge to gamble. A technique that allows the measurement of connectivity is dynamic causal modelling (DCM). Piray et al. (2015) used this technique to show that the modulation of dopamine in the connectivity from the ventral to the dorsal striatum correlates with trait impulsivity in healthy individuals. Their results inspired the question whether people who have an addiction disorder such as GD would show a similar effect in the interplay of both subdivisions of the striatum, and whether this effect could potentially be stronger and more sustained, to the point of it showing in endogenous connectivity differences and not as modulatory effects. We used resting-stated data of 37 patients with GD and 37 HCs to test whether people with GD exhibit a higher endogenous connectivity from the ventral to the dorsal striatum in DCMs. Additionally, we also tested whether the strength of this connectivity correlates with BIS scores of trait impulsivity. Our results did not confirm these hypotheses, since there were no group differences in connectivity from the ventral to the dorsal striatum between GD and HCs, nor a significant correlation of the connectivity parameters with BIS scores. Future research should investigate whether potential connectivity differences are found during dynamic tasks rather than in rest, as we measured here.

Contents

Chapter 1

Introduction

1.1 Background and hypotheses

Gambling disorder (GD) is a clinical condition characterized by persistent gambling by an individual associated with impairment to other areas of their life (Potenza et al., 2019). The DSM-5 classifies GD together with substance use disorder (SUD) as an addiction disorder. This is because many traits of addiction are observed in the behavioral patterns of those who suffer from GD. They often report greater needs to gamble with higher amounts of money to achieve the same level of excitement as before, and also face psychological distress similar to withdrawal symptoms, which makes it harder for them to stop gambling (American Psychiatric Association, 2013). These similarities render GD as a key mental disorder for deepening our understanding of addiction: the mechanisms behind GD portray how addictions can be developed on a purely behavioral level, without the use of neurotoxins, as is with SUDs. Thus, potential neuronal alterations found in GD could tell us how addictions overall develop in the brain. The current study focused on studying striatal connectivity in GD in comparison to healthy populations.

The main system known to be affected in GD is the reward system (Zack et al., 2020). This system is responsible for associating valence and salience of stimuli to actions made to obtain it, as well as keeping track of these values so that the organism is able to predict the outcome of future actions (Arias-Carrión et al., 2010). In this way, one can learn how to obtain valuable resources from the environment. This process is implemented in the brain mainly in frontostriatal circuits, with a relevant role being played by dopamine as a signalizer of such values (Daw & Tobler, 2014). While SUDs chemically alter the structure of this system (Clark et al., 2019), the mechanism stipulated for behaviors to become addictive lies on the unpredictability

of reward. When a clear association between stimulus and reward cannot be achieved, the dopaminergic system sustains elevated levels of activity due to a high predictive error signal (Fiorillo et al., 2003). Gambling is an activity where uncertainty over the outcome is inherent, and thus capable to sustain such elevated levels of activity in the frontostriatal areas. This can lead to a hyper- or hyposensitization of these areas to the dopamine signal, which in turn would lead to addiction (Potenza et al., 2019; Zack et al., 2020). Researchers who favor the hypersensitization account postulate that the brain of those who develop an addictive disorder is naturally at a lower level of dopamine, which leads these people to seek more intense reward stimuli than natural ones such as food or sex, to achieve enough excitation of the reward system. Meanwhile, researchers who favor the hyposensitization account postulate that while there is no natural difference in the levels of dopamine before the development of an addiction, the continued exposure of the reward system to intense stimuli conditions it to reduce its general reactivity, leading to addictive behavior to sustain enough activation of the system (Limbrick-Oldfield et al., 2013).

One key brain area in the reward system is the striatum. There is evidence that the striatum plays three different roles with its subdivisions, a motivational one, a cognitive one, and a motor one (Aarts et al., 2011; Alexander et al., 1986; Haber & Knutson, 2010). The motivational functions of the striatum are said to be mainly implemented in the ventral striatum, where learning of stimulus-outcome pairings take place. This area would then be responsible for giving a person the impulse to take an action at the presence of determined stimuli. Meanwhile, the other two roles of the striatum are said to be located in its dorsal area, which means that both inhibition of impulses that are then deemed to be unhelpful to the organism and the motor planning for the execution of the same impulses when they are not inhibited take place in this region.

A reference study in the connectivity of the striatum and dopamine action within it is Piray et al. (2015). To investigate how dopamine modulates intrinsic striatal connectivity in healthy individuals, Piray et al. administered both a dopamine receptor agonist (bromocriptine) and an antagonist (sulpiride) to participants, which then conducted a reversal learning task, described in Van Der Schaaf et al. (2014), under the effect of the drugs while fMRI scans of their brain activity were recorded. To identify which subareas of the striatum were functionally correlated, they applied a k-clustering algorithm, which resulted in three VoIs: the ventral striatum (VS), the dorsal caudate nucleus (DCN) and the dorso-anterior putamen (DAP). After this identification, they used a technique called dynamic causal modelling (DCM) to estimate the baseline connectivity between these areas and the modulation

that the drug application would cause.

In their study, Piray et al. found that the connection from the VS to the DCP showed a consistent modulatory effect based on the administered drug. Namely, the connection was intensified by the administration of a dopamine agonist, while it was lessened in the presence of the antagonist. Furthermore, this modulatory effect exhibited a positive correlation with trait impulsivity, meaning that the more impulsive a participant was, the stronger the effect appeared in both ways: the connection was even more intensified by the administration of an agonist, while it was further lessened down in the presence of the antagonist. These results were interpreted as an indication of how the areas associated with the cognitive functions of the striatum can fall prey to the areas associated with motivational aspects. Higher impulsivity correlates with higher influence of motivation onto cognition, which can be seen as a failure at inhibition.

The link of such modulation with impulsivity is essential for us, since it plays a key role in understanding GD: it is known that those who suffer from it also tend to score high in trait impulsivity measures, such as the BIS/BAS scales (Carver & White, 1994). This is the main reason why the dopaminergic action in the striatum, especially in the interaction between its ventral and dorsal areas, is a focus of research in the literature of GD's neurobiology. This is also the focus of the current study.

While most fMRI studies use methods that compare the level of activation in certain areas between groups, they do not take connectivity between areas into account. Mapping of white matter in GD compared to healthy populations show more significant deterioration on many tracts (Joutsa et al., 2011; Mohammadi et al., 2016; Yip et al., 2017), including the basal ganglia to frontal cortex tract (Van Timmeren et al., 2017), which is more associated with reward processing (Daw & Tobler, 2014). How these differences are linked to the symptoms of GD is still unknown, but they could be a signal of a potential alteration in the connectivity pattern between these areas. Considering that the brain is interconnected, activation patterns in one region also affect how other regions behave. These dynamics are important to untangle in order to achieve a more holistic understanding of the mechanisms behind reward processing.

Inspired by Piray et al. (2015), whose methodology allows the understading of directional connectivity and its modulation, with findings already involving the dopaminergic system, we set forth to explore whether a similar effect could be observed in GD. Could it be that the modulation effect found by Piray et al. (2015) becomes a chronic, stable signal in patients with GD due to their higher impulsivity and high exposure to behaviors that exploit such impulsivity, to the point it is observed in the endogenous connectivity

between the ventral and the dorsal striatum? Additionally, it was reported that the modulatory effects of the drugs were stronger in highly impulsive participants, but could it be that this strength was due to a predisposition due to higher endogenous connectivity in these same people?

These indications led to the following hypotheses being put to test over the available resting-state fMRI dataset at the lab: is there a higher connectivity to the dorsal striatum from the ventral striatum in GD patients compared to HCs when measured through a DCM model? Is the intensity of this connectivity positively correlated to trait impulsivity?

To tackle these questions, we decided to combine methods already established in the lab with Piray's work. Before conducting the analyses described further in the report, we also pre-registred the study under OSF. This pre-registration can be found under Van Holst and Boger (2024), or at https://osf.io/mc4jt.

The resulting procedure was a resting-state DCM analysis described in the next chapter and an online repository available at: https://github.com/mathboger/amc-uva-internship-2024. There it is possible to find more detailed specifications of parts of the data as well all scripts that were utilized for the project. However, for privacy reasons, the scans, raw or preprocessed, utilized in this research project are not made public.

1.2 Practical considerations

A focus on GD was chosen for this project for practical reasons. As part of the Research Master's Brain and Cognitive Sciences (MBCS) of the University of Amsterdam, a personal goal was set to acquire experience with analyzing brain data, even better if it was connected to cognitive modelling and mental health issues, since these are of interest to the author. Since the supervisor of the project already had scans that needed this type of analysis of patients with GD, the expectations aligned and the focus was set. Also because of program requirements, a data collection on gambling and gaming behavior in young adults in the Netherlands was conducted, again for practical reasons. It is required to the students of the program that through one of the two research projects they conduct data collection. Originally, the author was going to be present at a scanning session of these gamblers. However, due to privacy concerns, this could not be arranged, and a similar type of collection was designed instead. Nonetheless, since this part of the project has a different scope than the rest, it is left as an appendix in this report.

Chapter 2

Methods

To achieve an understanding of the striatal connectivity in GD, we first collected the scans from the patients and HCs and combined them into one dataset. This is the first section on this chapter: the scanning procedure and the dataset structure. Then, we preprocessed the data (second section) to have a clean input for the DCM (third section). Finally, group level comparisons were conducted through PEB (parametric empirical Bayes) models (fourth and final section).

2.1 Scanning and the dataset

First of all, it is important to note that the data used in this project was originally collected at two different points in time, with the same procedure, for two different other projects in the lab. These were mainly conducted by Monja Hoven (Hoven et al., 2022) and Tim van Timmeren (Van Timmeren et al., 2023). In this report and the scripts attached to it, they are referred by Monja and Tim's names or as dataset 1 and dataset 2 (being these Monja's and Tim's, respectively). It is good to note that for the aforementioned projects, the scans that were utilized for the analyses were functional scans during a task, while in this research project we ran analyses over the resting-state scans that were not analyzed previously. This means that the whole preprocessing pipeline was readjusted for these scans, and the final mask extraction for the DCM was chosen to be as close as possible to Piray et al. (2015).

In total, Monja's dataset included 31 people with GD and 49 HCs. Of these, 16 patients and 12 HCs had to be discarded due to saving errors in the resting-state data. As for Tim's, we had 22 patients and 3 HCs available, none discarded. All the available resting-state data passed the motion control test

of not having the participant move more than one voxel during the recording session. For brevity, the motion parameters and the correspondent plots are available at the online repository of this project and omitted here. In the end, we have in total then 37 people with GD, of which 8 women, and 40 HCs, of which 15 women, represented in the data. To make the number of patients and controls match, we randomly discarded 3 controls, of which 1 woman, and ran the subsequent analyses only on the patients and the selected controls.

To guarantee we had a representative sample of HCs to match the patients, we ran a demographic analysis before preprocessing the data. Using Wilcox signed ranked tests for numeric data and chi-squared tests for categorical data, we found no significant differences in the distributions of age, gender, education level and alcohol use level as measured by the AUDIT scale. Significant differences were found for gambling severity index as measured by PGSI (ever, p=2.55e-15, now, p=2.47e-15) and trait impulsivity as measured by BIS/BAS scales (BIS, p=0.006, BAS, p=0.0003, BAS drive score, p=0.71, BAS fun seeking score, p=0.12, BAS reward responsiveness score, p=2.5e-11), which were expected due to the nature of the patient population. A brief overview of the demographic data is available in Table 2.1.

The fMRI scanning, as reported in Van Timmeren et al. (2018), was done in a 3 Tesla full-body Philips Intera MRI scanner, with a 32-channel phased array SENSE radiofrequency receiver head coil. T2*-weighted gradient multi-echo echoplanar images were acquired with repetition time (TR) of 2375 ms, and echo times (TEs) of 9, 26.4 and 43.8 ms. The flip angle was 76°, with a field of view (FOV) of 224 x 121.8 x 224 mm, voxel size of 3 x 2.95 x 3 mm, matrix size of 76 x 73, slice thickness of 3 mm, slice gap of 0.3 mm, totaling 37 slices acquired in interleaved order. For Monja's dataset, 255 scans were acquired per participant, while Tim's dataset includes only 200 scans per participant. For this reason, we discarded the final 55 scans from Monja's data when including it in the DCM analysis.

2.2 Preprocessing

Preprocessing of the data was done with the SPM12 package for MATLAB (Friston, 2007). Most of the standard pipeline of SPM was kept, with slight alterations, mainly in voxel and smoothing kernel size, to fit the data better as already conducted in Hoven et al. (2022). The exact job script is available at the online repository, but an overview of the settings follows.

Realignment: Estimation options with quality of 0.9 out of 1, separation

Table 2.1: Demographic overview of the dataset. Mean and standard deviation reported for numeric data.

	GD	HC
Total number	37	37
Number of women	8	15
Education level: elementary school	0	0
Education level: secondary school	9	14
Education level: middle-level applied education	22	10
Education level: higher professional education	6	7
Education level: scientific education	0	6
Age (years)	33.2 (11.9)	37.0 (14.6)
AUDIT	4.68 (4.87)	3.16 (2.10)
PGSI (now)	15.54 (3.85)	0.00 (0.00)
PGSI (ever)	14.54 (4.07)	0.00 (0.00)
BIS	19.27 (3.02)	17.03 (3.69)
BAS (total)	43.27 (4.81)	38.14 (5.63)
BAS (drive)	12.65 (2.30)	12.51 (2.39)
BAS (fun seeking)	12.35 (2.15)	11.38 (2.63)
BAS (reward responsiveness)	18.27 (1.67)	14.24 (1.66)

of 4 mm, smoothing kernel of 5 mm, registration to the mean, interpolation calculated by 2^{nd} degree B-spline, no wrapping and no additional weighting image. Reslicing options to reslice all images and generate a mean image, with interpolation calculated by 4^{th} degree B-spline, no wrapping and masking set to on.

Coregistration: Reference image set to the mean image from the reslicing step, applied to all images with estimation options of making using of normalized mutual information for the object function, with separation of 4 and 2 mm, 12 iterations where the first 3 steps have an accuracy tolerance of 0.02 and then 0.001 for the others, with histogram smoothing kernel of 7 by 7.

Segmentation: The standard SPM tissue maps were used to segment the recording into six types of tissue (grey matter, white matter, CSF, bone, soft tissue and air), however only the full image was kept. Light bias regularization of 0.001 was applied with a 60 mm cutoff, which was saved. Warping was conducted with Markov random field (MRF) clean-up parameter of 1, light clean, affine regularization parameters of 0, 0.001, 0.5, 0.05 and 0.2 to European brains (per available in SPM), smoothness of 0 mm, sampling distance of 3 and forward deformation fields.

Normalization: Applied to the forward deformated images from the segmentation step, written to the bias corrected ones. Bounding box of -78x-112x-70;78x76x85 mm, voxel size of 3x3x3 mm, interpolation calculated by 4^{th} degree B-spline.

Smoothing: Kernel of 6 by 6 by 6 mm, keeping the same data type as the original images with no implicit masking.

Finally, the preprocessed images were masked in order to extract 3 different RoIs for our study. Based on the clusters found by Piray et al. (2015), we opted to link their VS node to the nucleus accumbens probability map as provided by the Harvard-Oxford atlas, the caudate nucleus probability map to the DCN of their study and the same for the putamen and DAP, both again from the Harvard-Oxford atlas. This decision was due to our concerns over the application of a heavily data-dependent method such as the k-clustering algorithm to brain parcellation, as it could make findings less stable since its exact outcome varies according to which exact participants were included in the dataset. In this way, all the equivalent models fitted in Piray et al. (2015) were fitted in this study too. This is the topic of the next session.

2.3 DCM

DCM consists of a modelling technique where the expected BOLD signal is calculated from connectivities established a priori between RoIs (Zeidman, Jafarian, Corbin, et al., 2019). The resulting signal is then compared with the actual observed signal to tune the parameters over the fitting procedure. Once the best fitting parameters are found for a model, the amount of data explained is compared to other postulated connectivity patterns to see which one presents the best fit. Generally, a fully connected model is also fitted as a baseline comparison. On top of the endogenous connectivities, task and procedure dependent modulations can also be added into the model, where new parameters are then fit to represent these additional dynamics. The endogenous connectivities are coded in what in the literature is referred to as the A matrix, while the signal tuning that results from the modulations are represented by the B matrix in the literature. It is good to note that the connectivities in DCM do not have to be symmetrical, which adds an element of directionality to the model, which is not possible through a simple correlation coefficient calculation. In this way, it is possible to more reliably untangle the degree to which the signal in one area varies dependent on the signal in another area, and make clear in which direction the modulatory effects take place.

As previously mentioned, all DCMs presented in Piray et al. (2015) had their equivalent model in our methodology also fitted. However, some alterations were necessary. This is because the data at hand for us is multi-echo resting-state scans. In SPM 12, DCMs only take one echo time (TE) as input to represent the TE of the scanning procedure. Thus, in our case, it is not clear which TE should be provided for either a better model fit or a more accurate representation of the scanning procedure. We decided to then fit variations of the same model with different TEs to establish empirically which TE to use based on model fit. For that, we used 4 different TEs. First, all 3 that were used in the procedure (9, 26.4 and 43.8 ms), and then a weighted average of 30.6 ms that takes into consideration the image combination procedure and tissue dependent relaxation time T_*^2 (Krüger & Glover, 2001; Poser et al., 2006).

Next, some changes were introduced due to the nature of resting-state data. In DCMs, there are many parameters that are fitted in order to replicate the final BOLD signal (Zeidman, Jafarian, Corbin, et al., 2019). These include the baseline connectivity between regions, as well task (or condition) induced modulations. Our data does not encompass such additional fluctuations, and so these parameters are all set to 0. In this way, only baseline connectivity is fitted and tested. Also because this task timing dependency is not a feature of resting-state data, we are able to fit the model in the frequency domain instead of the time domain (Ashburner et al., 2021). This technique is referred to as spectral DCM, and it is recommended when comparing the endogenous coupling of different brain areas in two or more populations in resting-state data, as we do in this study. This makes the whole model simpler to understand and compare, since now all the neuronal parameters that are fitted represent only this (directional) endogenous connectivity. In the DCM literature, these parameters are represented as the elements of the A matrix, where columns and rows represent the different RoIs of the model and an element represents the connectivity from the row to the column (so a_{12} would be the connectivity from area 1 to 2, while a_{21} is the one from 2 to 1, note however that SPM sets the model with the opposite orientation, so a transposition would be necessary). These are the parameters over which we investigate a population based difference between people with GD and HCs, as well as a correlation between those and BIS trait impulsivity scale outcomes.

As such, the specifications for our models were the following (also available in the online repository as a script): GLM as described below, VoI 1 for the nucleus accumbens, VoI 2 for the caudate nucleus, VoI 3 for the putamen, all VoI timings equal to TR of 2.375 s, TE varied as explained previously, being either 9 (TE1), 26.4 (TE2), 30.6 (TE3), or 43.8 ms (TE4), bilinear

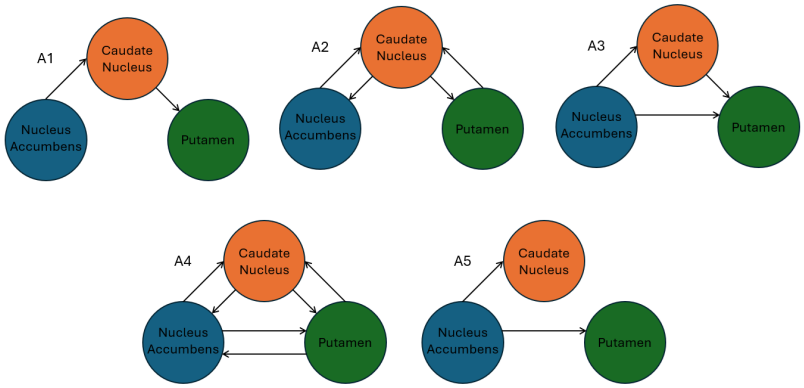

Figure 2.1: Schematic representation of the connectivity matrices fit for each DCM model. The self-connections of each area onto itself are omitted in the figure, but present in the model.

modulatory effects, one state per region, no stochastic effects, centred input, fit for CSD, A matrix varied from A1 to A5 to represent the schemes found in Figure 2.1, and full 0s for matrices B, C, and D. The A matrices are the same from Piray et al. (2015).

Finally, the GLM we used to reference the participants listed them in an ascending order of registration code, taking first all patients from dataset 1, then all patients from dataset 2 (so participants 1 to 37 are all the patients), and then all HCs from dataset 1, then all HCs from dataset 2 (so participants 38 to 74 are all HCs). No extra confounding factors were added to the GLM that serves as input to the DCM since we had already established that the samples were demographically well controlled.

Since we varied between 5 different connectivity matrices and 4 different TEs per participant to see which model was best, we had 1480 models in total to fit (20 models per participant). To choose the best combination of TE and A, we opted to look at the sum of the BIC value output by SPM over all participants over a specific combination. The model with the lower BIC was chosen to undergo further analyses with PEB, the final section of our methods.

2.4 PEB

The last step needed to test whether there is a group effect in the connectivity from the ventral striatum to the dorsal is to do a second level analysis.

This can be done through PEB analysis, also available in SPM 12, for which a succint explanation on how this method works can be found in Zeidman, Jafarian, Seghier, et al. (2019). This Bayesian method allows for an estimation of how much each group's mean diverge from the overall mean and an evaluation of that effect through model pruning.

Following the setup we used for the GLM, we added the PEB covariate 'Group' to indicate with a 1 that participants 1 to 37 are patients and with a -1 to indicate that participants 38 to 74 are HCs. The fit PEB model would later go through a model reduction analysis in order to establish if adding group effects to the mean increases model explanation power as taken by a 95% posterior probability of such parameter being present rather than absent when thresholded based on model free energy. An effect due to having the diagnosis of GD is considered to exist if the relevant parameter is still included in the reduced model after this analysis. Additionally, a leave-one-out (LOO) analysis of establishing whether a new participant can be classified into the GD or HC groups based on its fit connectivity matrix given all the other participants' matrices is also run. If the reduced model shows differences between these groups, such classification should be possible.

We ran the PEB analysis with all standard settings of SPM 12, with the exception to increasing the maximal iterations to 256. The field of interest was set to matrix A, since we are looking at the endogenous connectivities between the areas.

Chapter 3

Results

To recap, we had 20 models per participant to fit, varying TE and connectivity hypothesis, to evaluate which model would better explain the data with the least amount of variables possible. To choose a combination of TE and connectivity matrix A, we compiled the sum over all participants of each model's BIC. This can be seen in Table 3.1.

Table 3.1: Sum of BIC over participants per TE and A combination.

	A1	A2	A3	A4	A5
TE1	-328960.2	-333751.9	-328567.9	-336091.8	-329278.9
TE2	-328960.2	-333751.9	-328567.9	-336091.8	-329278.9
TE3	-328960.2	-333751.9	-328567.9	-336091.8	-329278.9
TE4	-328960.2	-333751.9	-328567.9	-336091.8	-329278.9

As can be seen, surprisingly enough there were no alteration of BIC values due to different TEs in model specification. We decided to run an analysis fitting multiple TEs into the models because we could not find in the DCM literature what is the most recommended practice when applying this methodology that takes into account a single TE value to scans that were acquired with multi-echo procedures. We did find a paper that made use of SPM's DCM package for multi-echo images (Hauw et al., 2023), and private correspondence with the author gave us insight that the setting of a specific TE is not relevant for model fit, which we were able to confirm. With this knowledge, we decided to do further analyses with TE2, 26.4 ms, because it is not only the median value of the 3 TEs in the scanning procedure, but also its arithmetic average. While we could opt for TE4, our theoretical weighted average based on the combination procedure, we concluded that it was best to not add further speculation on top of an used input value if a simpler option was perfectly equivalent when it comes to model fit.

As for the connectivity matrix A, we found that A4, the fully connected model, had the best fit. Accordingly, the model chosen for further analyses was A4TE2. Additionally, we also decided to run similar analyses on model A2TE2 because it is the model that showed best evidence in Piray et al. (2015) and still second best fit in our study.

As for model A4TE2, when taken to the group level with PEB analysis, the results did not corroborate our hypothesis. In other words, we were not able to find a group related difference in the connectivity from the ventral to the dorsal striatum. Fitting the simple PEB showed a higher than 95% probability of a group effect being present for the majority of the connections, but when a model reduction analysis was run to take also the covariance between the variables into account, no single connectivity difference per group withstood the 95% mark in free energy variation. This means that while the model fitted with values that are significantly different than 0, the addition of these parameters to the model did not increment its applicability in understanding the data, which favored the adoption of the null hypothesis. This information is compiled in Figures 3.1 to 3.3. Finally, running a leave-one-out validation analysis also led to most classifications resulting in chance level at around 50% probability, as can be seen in Figure 3.4. This once again confirmed that no substantial difference in connectivity can be observed between the two groups from the ventral to the dorsal striatum under resting-state.

Similar results held for A2TE2, which can be seen in Figure 3.5 for the PEB model, Figures 3.6 and 3.7 for the reduction analysis and Figure 3.8 for the leave-one-out classification.

As for the correlation analysis, where we hypothesized a significant positive correlation between the connectivity from the ventral to the dorsal striatum with trait impulsivity scores, we tested for BIS scores when correlated to both connections from the nucleus accumbens to the caudate nucleus and from the caudate nucleus to the nucleus accumbens without making a discrimination if the participant was a patient or a HC to capture the whole range of the impulsivity trait measures. The results indicated no significant correlation. A compilation of the correlation values are given in Table 3.2. Plots were omitted for brevity, since the correlations were not significant and they can be easily reproduced with the scripts available in the online repository.

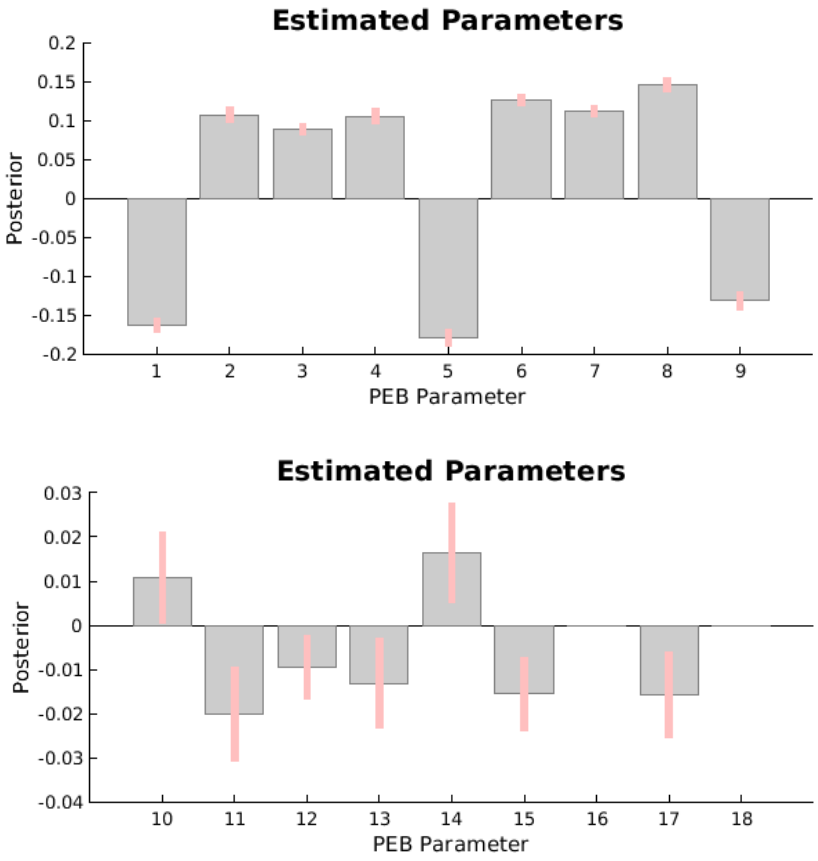

Figure 3.1: Value and 95% confidence interval of each PEB parameter of model TE2A4. Only parameters that did not include 0 in their confidence interval are shown. Parameters 1 to 9 plotted on the graph on top represent the commonalities, i.e., the mean value over both groups, while parameters 10 to 18 plotted on the graph on the bottom represent the group differences, i.e., the divergence from the mean connectivity depending on whether a participant is a patient (group 1, positive divergence) or a HC (group 2, negative divergence). Parameters 1 and 10 are the self-connectivity of the nucleus accumbens, 2 and 11 are the connection from the nucleus accumbens to the caudate, 3 and 12 are from the nucleus accumbens to the putamen, 4 and 13 are from the caudate to the nucleus accumbens, 5 and 14 are the self-connectivity of the caudate, 6 and 15 are from the caudate to the putamen, 7 and 16 are from the putamen to the nucleus accumbens, 8 and 17 are from the putamen to the caudate, and 9 and 18 are the self-connectivity of the putamen. It can be seen that a simple fit of the model gives a significant non-zero fit to almost all parameters before a reduction analysis is run.

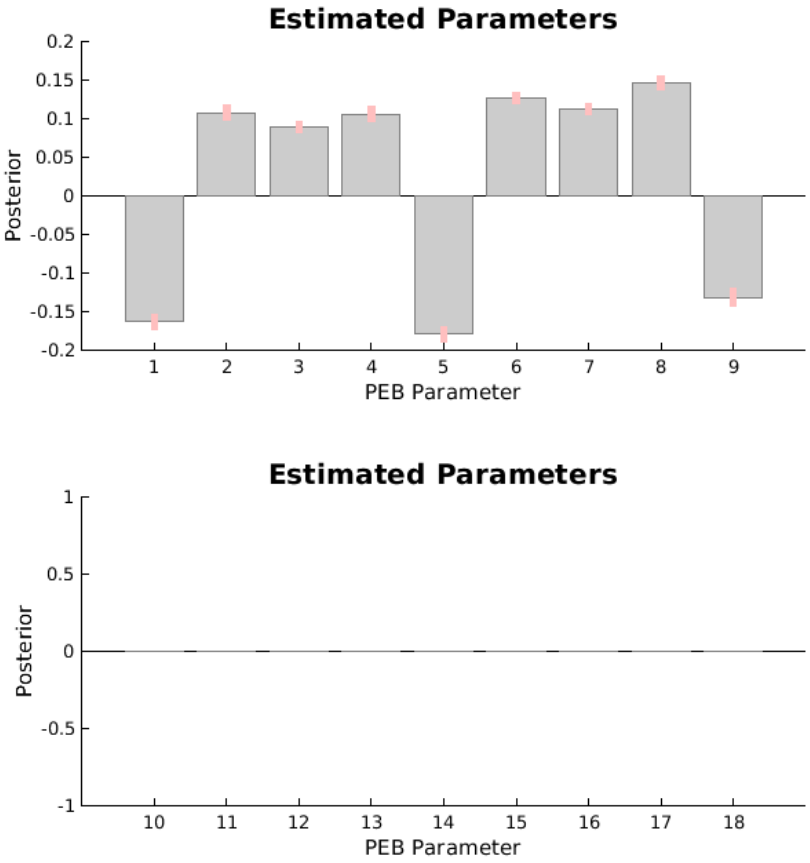

Figure 3.2: Value and 95% confidence interval of each PEB parameter of model TE2A4 after model reduction via free energy has been applied. Only parameters that did not include 0 in their confidence interval are shown. The numbering of the parameters follow the same pattern as in Figure 3.1. It can be seen that all group distinctions are lost, indicating there is no difference in the connectivity of these areas between people with GD and HCs. All the commonalities stay significant, confirming that these areas are indeed connected, in accordance to the literature.

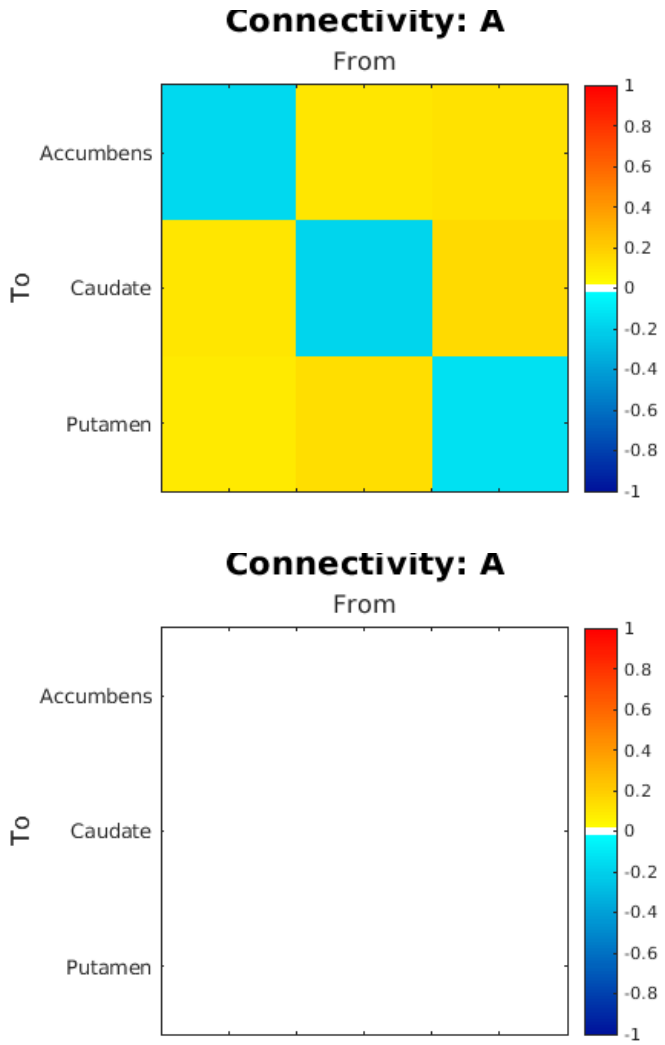

Figure 3.3: The same information from Figure 3.2 presented in matrix form for easier visualization. The top matrix refers to the commonalities, while the bottom matrix refer to the group effect. The empty bottom matrix reflects the reduction to zero of the group effects after reduction analysis. It is interesting to notice that all regions have mainly excitatory connectivities with each other, while having an inhibitory connectivity to itself.

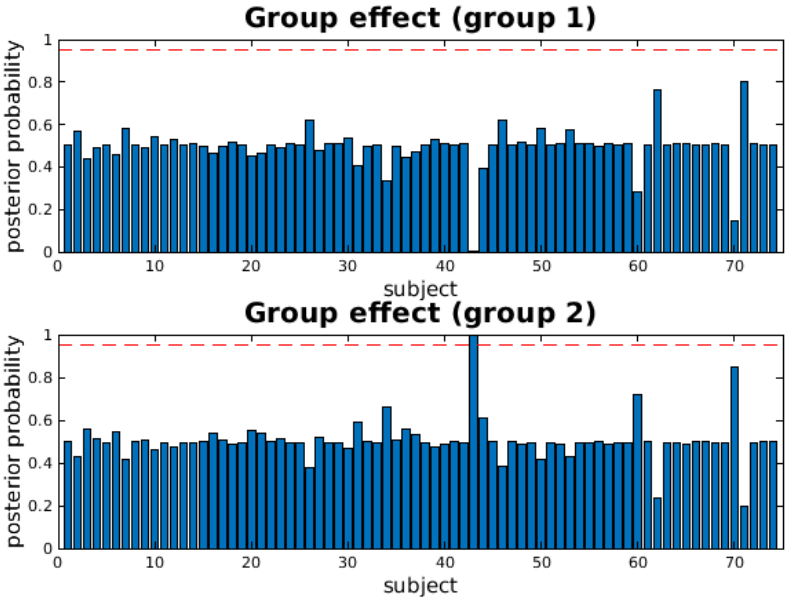

Figure 3.4: Leave-one-out classification attempt done with model TE2A4. Participants 1 to 37 are patients, and should be classified to group 1, while 38 to 74 are HC and should be classified to group 2. As can be seen, almost all participants show chance level classification. This is in line with the other results that there is no difference in the connectivities between the two groups.

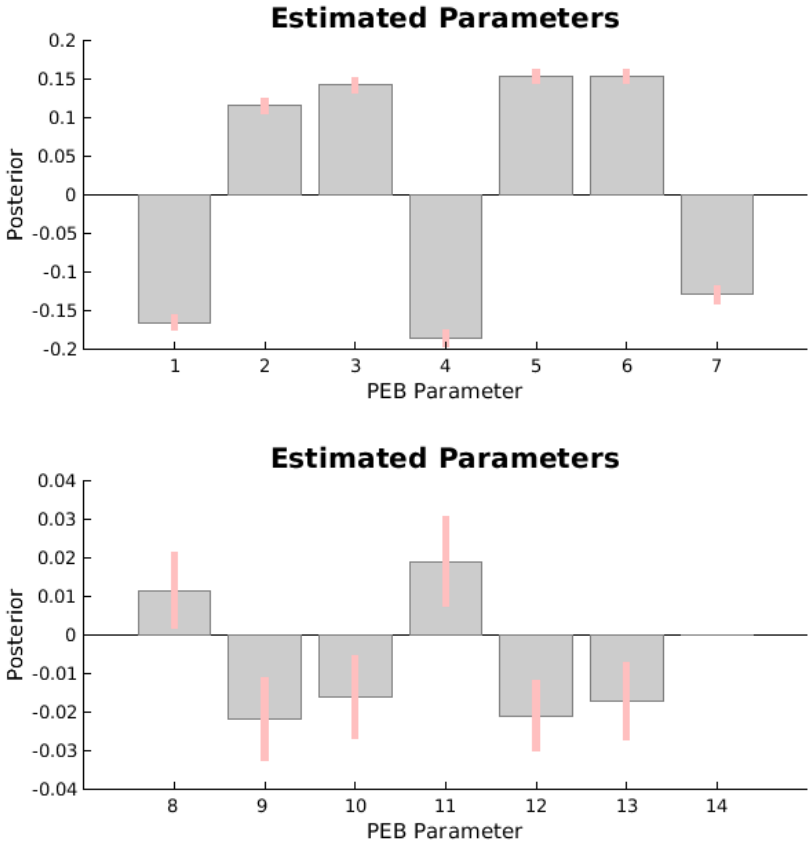

Figure 3.5: Value and 95% confidence interval of each PEB parameter of model TE2A2. Only parameters that did not include 0 in their confidence interval are shown. Parameters 1 to 7 plotted on the graph on top represent the commonalities, i.e., the mean value over both groups, while parameters 8 to 14 plotted on the graph on the bottom represent the group differences, i.e., the divergence from the mean connectivity depending on whether a participant is a patient (group 1, positive divergence) or a HC (group 2, negative divergence). Parameters 1 and 8 are the self-connectivity of the nucleus accumbens, 2 and 9 are the connection from the nucleus accumbens to the caudate, 3 and 10 are from the caudate to the nucleus accumbens, 4 and 11 are the self-connectivity of the caudate, 5 and 12 are from the caudate to the putamen, 6 and 13 are from the putamen to the caudate, and 7 and 14 are the self-connectivity of the putamen. It can be seen that a simple fit of the model gives a significant non-zero fit to almost all parameters before a reduction analysis is run.

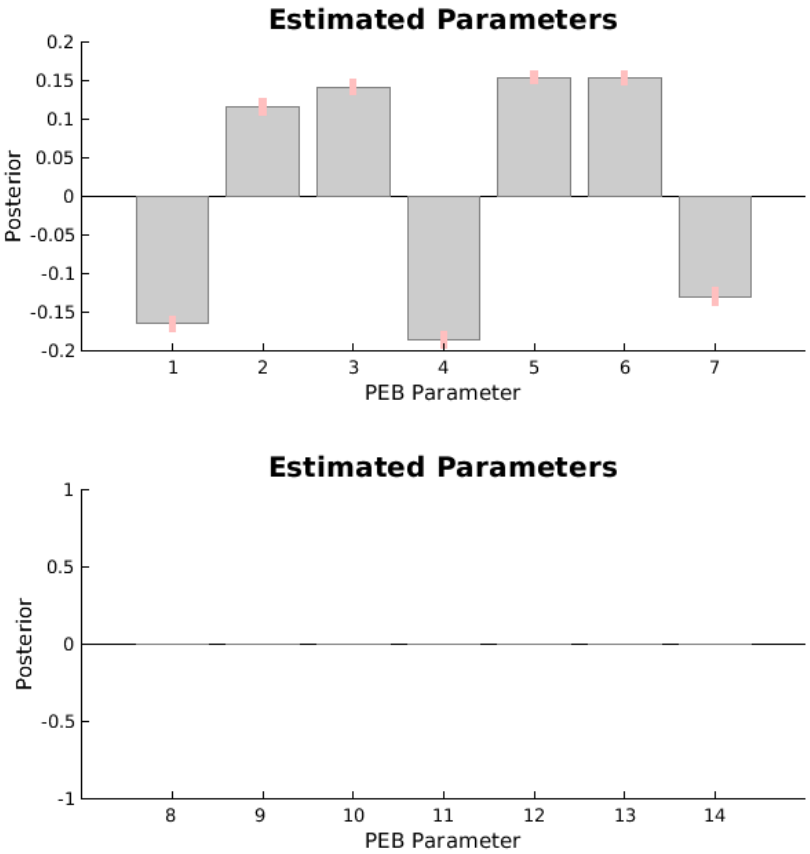

Figure 3.6: Value and 95% confidence interval of each PEB parameter of model TE2A2 after model reduction via free energy has been applied. Only parameters that did not include 0 in their confidence interval are shown. The numbering of the parameters follow the same pattern as in Figure 3.5. It can be seen that all group distinctions are lost, indicating there is no difference in the connectivity of these areas between people with GD and HCs. All the commonalities stay significant, confirming that these areas are indeed connected, in accordance to the literature.

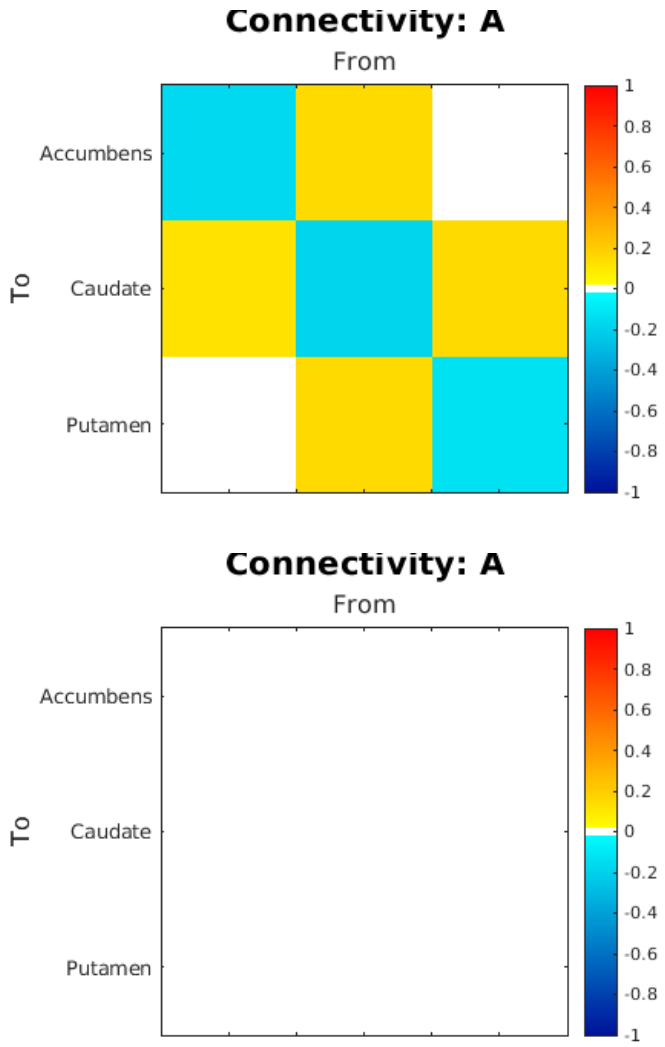

Figure 3.7: The same information from Figure 3.6 presented in matrix form for easier visualization. The top matrix refers to the commonalities, while the bottom matrix refer to the group effect. The empty bottom matrix reflects the reduction to zero of the group effects after reduction analysis. It is interesting to notice that all regions have mainly excitatory connectivities with each other, while having an inhibitory connectivity to itself. The empty squares on the top matrix show connections that were turned off in the definition of the model.

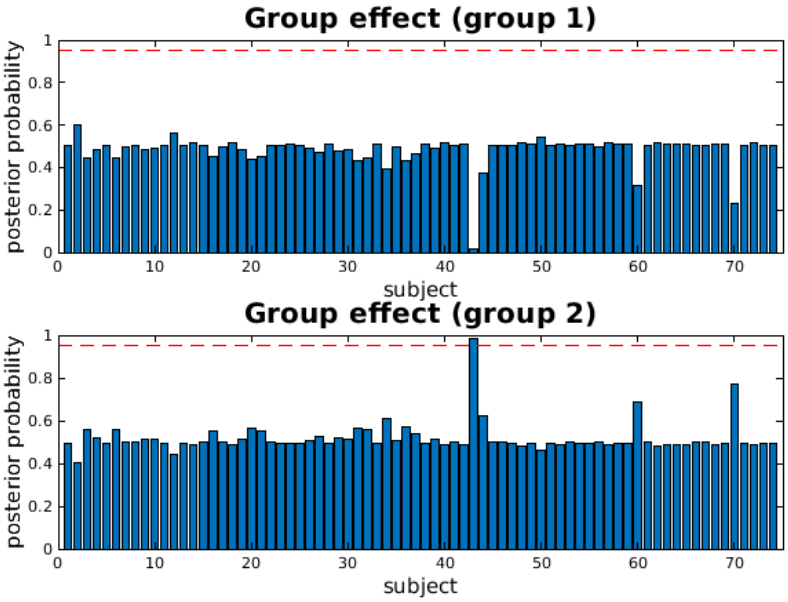

Figure 3.8: Leave-one-out classification attempt done with model TE2A22. Participants 1 to 37 are patients, and should be classified to group 1, while 38 to 74 are HC and should be classified to group 2. As can be seen, almost all participants show chance level classification. This is in line with the other results that there is no difference in the connectivities between the two groups.

Table 3.2: Correlation observed between trait impulsivity measures and fit connectivity values.

	Nucleus accumbens to caudate nucleus	Caudate nucleus to nucleus accumbens
BIS	-0.20 (p=0.08)	-0.15 (p=0.21)

Chapter 4

Discussion and conclusion

Based mainly on the findings and methods of Piray et al. (2015), we hypothesized an increase in the connectivity from the ventral to the dorsal striatum between people with GD and HCs. This is because we expected that the higher dopaminergic modulatory effect observed in more impulsive people would be in line with the higher impulsivity found in people with GD. We also hypothesized that the same connectivity would be positively correlated with the BIS measures of trait impulsivity of the whole participant population, since the original modulatory effect was also stronger as impulsivity rose. Our results did not confirm our hypotheses.

We did not observe a difference in the connectivity parameters from the ventral to the dorsal striatum between HCs and patients, nor a positive correlation between this connection and trait impulsivity as measured by the BIS scale. Regarding the models, our Bayesian approach would have allowed us to detect results in the opposite direction as hypothesized, but they were in fact null. This simplifies the interpretation of what our results could mean, since they state there is no difference between the two groups in any direction.

This finding also aligns with literature when we look at other task-independent measures in the brain. Structurally speaking, the data for gray matter deficits in GD is inconclusive (Clark et al., 2019), as brain-wide scans show no statistically signficant alteration for GD (Joutsa et al., 2011; Van Holst, De Ruiter, et al., 2012), while some size alterations appear both ways when focus is placed on specific regions (Koehler et al., 2015; Zois et al., 2017). PET studies also suggest that there is no difference in the amount of dopamine receptors between HCs and people with GD (Boileau et al., 2013; Clark et al., 2012). This information suggests that the baseline cognitive processing and dopaminergic connectivity of people with GD is equivalent to HCs. If so, it is plausible to detect similar levels of connectivity as measured by the DCM

during rest.

Neverthelesss, this still begs the question if such differences do appear in a more dynamic environment, and if so, exactly why and how those differences come about. Traditional fMRI studies that do not use DCM generally only compare the levels of activations of a certain region, without measuring connectivity. It is then relevant to apply this methodology to fMRI studies that use tasks to test whether an altered pattern of activation then appears. If so, we are still left with the question of how can a system that in its static form shows no deviation from HCs display clinically impactful differences when dynamics come into play? One hypothesis could be that a gambling related task could elicit higher levels of dopamine in the area, causing a greater modulatory effect, such as the one observed in the agonist condition of Piray et al. (2015). Alternatively, one could look further down or upstream in the reward system chain and additionally take into account frontostriatal connections as well as connections to the dopamine producing areas of the midbrain (Roeper, 2013).

On the other hand, comparison of GD to SUD might be productive as well. Originally we had also hoped to include in this study, in case time allowed, an additional examination between the resting-state of the populations of the current study to people with alcohol use disorder (AUD). We had thought of AUD as a common representative of a SUD, which are disorders also linked to impulsivity, but include the neurotoxic effect of drugs reshaping neuronal activity, which even leads to a clear deterioration in gray matter (Rosenbloom & Pfefferbaum, 2003; Van Holst, De Ruiter, et al., 2012). It could be that a resting-state effect similar to the one found in Piray et al. (2015) is only observable in populations with supranatural doses of dopamine and its long-term effects on striatal connectivity.

Fortunately, the lab already has the same type of data, under the same scanning procedure, of participants with AUD, and the scripts for such preprocessing and testing are available as the product of the current study. It should be a matter of time for the same questions to be answered, positive or negatively, for this population. Alternatively, one could think of possible cognitive tasks that could elicit different behaviors between people with GD and HCs, so that the aforementioned dynamic differences hypothesis could be tested. These tasks would most likely be akin to gambling (such as risky decision making, for example), if not gambling itself. Previous studies have shown already that such tasks elicit different levels of activation in the brain areas more associated with GD (Clark et al., 2019). Those that resemble gambling with a slot machine elicited higher activation in the ventral striatum for reward anticipation and lower for sequential near-miss loss (Sescousse et al., 2016; Worhunsky et al., 2014), while a card-guessing task

elicited higher activation in the dorsal striatum (Van Holst, Veltman, et al., 2012). However, these studies do not use DCM technology, and thus only testified different levels of activation, and not connectivity, which remains to be tested.

Additionally, our null findings also in comparison with Piray et al. (2015) should be interpreted in light of some key differences between the latter and the current study. For ease of comparison, these are compiled in Table 4.1. Briefly put, we used resting-state fMRI while they had a task-based fMRI, we compared a group of people with GD to HCs while they only had healthy individuals in their cohort testing for different drug effects, we looked only at endogenous connectivity while they looked at modulatory effects, and we used pre-made masks for VoI extraction while they used k-clustering.

Table 4.1: Main differences between the current study and Piray et al. (2015).

	Current study	Piray et al. (2015)
Type of scanning	Resting-state fMRI	fMRI with a task
Difference in conditions	Group (HC or GD)	Dopamine (ant)agonistic administration
DCM parameter analyzed	A (endogenous connectivity)	B (modulation by condition)
Definition of VoI	Masks	k-clustering
Model fit criterion	BIC	Exceedance probability

While we had grounds to believe that their findings could be reproduced in our data in case that the dopaminergic connections in the striatum were structurally different in baseline GD brain behavior because of higher impulsivity levels, it turned out that this was not the case. The difference in conditions between the two experiments cannot be overcome, since we did not administer any drugs due to our interest in the natural, resting-state behavior of both populations. Furthermore, when it comes to VoI definition, we utilized masks that encompassed the whole of the striatum separated into three subareas, while Piray et al. (2015) used a k-clusters algorithm that output five different clusters, of which three were hand-picked per participant to represent what is more consistent with the literature regarding the functional subdivisions of the striatum. This discrepancy in methodology means that their VoIs were smaller and perhaps more precise than ours, which could have enhanced the effect observed on their study. On the other hand, k-clustering is heavily dependent on the input data, and can show inconsistent outputs on the same participant depending on which total population it is run over. This can be tricky if you have two diagnostically different populations as in our case, because if the hypothesis predict that the base connectivity between the populations is different, it is hard to judge whether the clustering that is done a priori the confirmation or refusal of the hypothesis should take that into account or not. Had we used k-clustering as well, would our results be

more valid if we had only clustered among HCs and replicated the results as a mask onto the patients, or should we have run the algorithm over the whole participant population? This is not a trivial question, and precisely this type of ponderation is what led us to opt for a masked VoI approach [1]. As for the model fit criterion, we believe this difference to be irrelevant, since the BIC is amply used in most of the literature and is a robust way to judge model fit. Nonetheless, the differences in the type of scanning and the parameters of interest are crucial. They reflect the biggest changes from their study to ours: turning from a task-based to resting-state recording. This issue ties back to the point made previously that it is possible that such differences only appear under the presence of a task that resembles gambling. Additionally, modulation and connectivity are not the same, not theoretically, and not in DCM modelling. Endogenous connectivity, as we have investigated in this study, refers to the baseline change in activity of an area based on the activity of another (or the same) area in a previous time point. On the other hand, modulation is the change in this rate of change from connectivity depending on the condition of the experiment. The former is modelled in the A matrix of DCM, while the latter in the B matrix (Zeidman, Jafarian, Corbin, et al., 2019).

In conclusion, we could not observe a significant difference in the endogenous connectivity from the ventral to the dorsal striatum between people with GD and HCs. Furthermore, no significant correlation between the strength of such connectivity in resting-state and trait impulsivity was found. As a possible next step for future research, we suggest that resting-state DCM analysis is tested on people with AUD to test whether long term dopaminergic effects caused by alcohol would lead to more differences in functional connectivity, as observed in Piray et al. (2015). Another possible path of research is to test whether there is a difference in connectivity in the striatum when a gambling task is present. This would indicate higher dynamic effects that come into play in GD and serve as new standing ground for unraveling the connection between behavioral addiction and cerebral alterations.

[1] We did, however, implement their algorithm and it is available on the online repository along with preliminary results of such clustering attempts.

Appendix

As mentioned in the Introduction, additional data collection for another project running in the lab was done to fulfill the MBCS program requirements. In this section, a brief explanation of that project is given, and the data collection role is then presented. Note that this disconnected approached had to be taken for two reasons: first, the data used in the main project was already collected before the addition of the author to the research team, and second, because privacy concerns at the clinic barred the presence of the author to accompany a similar scanning session with patients.

This complementary data collection step concerns a recently approved project regarding gambling issues in the Dutch youth. Not much information about it can be disclosed at the current moment. However, one of the main goals of the initial phase stipulated by the stakeholders is to acquire information over the susceptibility and risk behaviors of the Dutch youth via online measurements of well-validated scales that comprise their tendency towards taking risks as well as new questions regarding the ever more prevalent gambling aspects in sports and videogames. To test this approach, we conducted a pilot study with 10 participants combining both Prolific and Qualtrics.

Prolific is an online tool that facilitates the distribution of studies to the right target population, guaranteeing that demographic requirements of a study are met with a representative sample. In that way, we were able to deliver the survey built in Qualtrics, the survey platform promoted by the University of Amsterdam, which included the assessments above, exclusively to young people aged between 18 and 24 that live in the Netherlands and speak Dutch as their first language.

To guarantee the quality of the data, a small check for each answer had to be done. Mainly because there are some open text questions in the survey, and one must check if the answers that were filled in were congruent with the scope of the questions, or even proper sentences to begin with. There were also questions in the survey regarding possibly problematic gaming and gambling behavior, which had to be congruent with the answers the participants

gave in other items. For example, if a participant reported not to game as a habit, they cannot report also perceiving relationship problems with their family and friends due to their gaming.

We used Prolific to run a pilot with 10 participants recruited from their pool. We were able to achieve this small number in the same day the pilot was released, and all participants were properly compensated for their time. The one issue that we noticed is that while we can target both language and age requirements, the same cannot be done for educational background. Part of the study that is set to run after this pilot is supposed to be targeted at MBO students, while the majority of the respondents from Prolific were from a HBO. This situation is planned to be solved by distributing the study through a network of people that would include staff members at MBO institutions.

Important to note here in this report is that the setup of the collection system and the quality check for the pilot were done in a timely and satisfactory manner, and the author had the opportunity to undergo a data collection experience to fulfill all the requirements from the program in order to graduate.

References

Aarts, E., Van Holstein, M., & Cools, R. (2011). Striatal dopamine and the interface between motivation and cognition. *Frontiers in Psychology*, *2*.

Alexander, G. E., DeLong, M. R., & Strick, P. L. (1986). Parallel organization of functionally segregated circuits linking basal ganglia and cortex. *Annual Review of Neuroscience*, *9*, 357–381.

American Psychiatric Association (Ed.). (2013). *Diagnostic and statistical manual of mental disorders: DSM-5* (5th ed). American Psychiatric Association.

Arias-Carrión, O., Stamelou, M., Murillo-Rodríguez, E., Menéndez-González, M., & Pöppel, E. (2010). Dopaminergic reward system: a short integrative review. *International Archives of Medicine*, *3*(1), 24.

Ashburner, J., Barnes, G., Chen, C.-C., Daunizeau, J., Flandin, G., Friston, K., Gitelman, D., Glauche, V., Henson, R., Hutton, C., Jafarian, A., Kiebel, S., Kilner, J., Litvak, V., Mattout, J., Moran, R., Penny, W., Phillips, C., Razi, A., ... Zeidman, P. (2021). *SPM12 Manual*. Functional Imaging Laboratory, Wellcome Centre for Human Neuroimaging.

Boileau, I., Payer, D., Chugani, B., Lobo, D., Behzadi, A., Rusjan, P. M., Houle, S., Wilson, A. A., Warsh, J., Kish, S. J., & Zack, M. (2013). The D2/3 dopamine receptor in pathological gambling: A positron emission tomography study with [11C]-(+)-propyl-hexahydro-naphtho-oxazin and [11C]raclopride. *Addiction*, *108*(5), 953–963.

Carver, C. S., & White, T. L. (1994). Behavioral inhibition, behavioral activation, and affective responses to impending reward and punishment: The BIS/BAS Scales. *Journal of Personality and Social Psychology*, *67*(2), 319–333.

Clark, L., Boileau, I., & Zack, M. (2019). Neuroimaging of reward mechanisms in Gambling disorder: an integrative review. *Molecular Psychiatry*, *24*(5), 674–693.

Clark, L., Stokes, P. R., Wu, K., Michalczuk, R., Benecke, A., Watson, B. J., Egerton, A., Piccini, P., Nutt, D. J., Bowden-Jones, H., & Lingford-Hughes, A. R. (2012). Striatal dopamine D2/D3 receptor binding in pathological gambling is correlated with mood-related impulsivity. *NeuroImage*, *63*(1), 40–46.

Daw, N. D., & Tobler, P. N. (2014). Value learning through reinforcement. In *Neuroeconomics* (pp. 283–298). Elsevier.

Fiorillo, C. D., Tobler, P. N., & Schultz, W. (2003). Discrete Coding of Reward Probability and Uncertainty by Dopamine Neurons. *Science*, *299*(5614), 1898–1902.

Friston, K. J. (2007). *Statistical parametric mapping: the analysis of functional brain images* (1st ed.). Elsevier.

Haber, S. N., & Knutson, B. (2010). The reward circuit: Linking primate anatomy and human imaging. *Neuropsychopharmacology*, *35*(1), 4–26.

Hauw, F., El Soudany, M., Rosso, C., Daunizeau, J., & Cohen, L. (2023). A single case neuroimaging study of tickertape synesthesia. *Scientific Reports*, *13*(1), 12185.

Hoven, M., De Boer, N. S., Goudriaan, A. E., Denys, D., Lebreton, M., Van Holst, R. J., & Luigjes, J. (2022). Metacognition and the effect of incentive motivation in two compulsive disorders: Gambling disorder and obsessive–compulsive disorder. *Psychiatry and Clinical Neurosciences*, *76*(9), 437–449.

Joutsa, J., Saunavaara, J., Parkkola, R., Niemelä, S., & Kaasinen, V. (2011). Extensive abnormality of brain white matter integrity in pathological gambling. *Psychiatry Research: Neuroimaging*, *194*(3), 340–346.

Koehler, S., Hasselmann, E., Wüstenberg, T., Heinz, A., & Romanczuk-Seiferth, N. (2015). Higher volume of ventral striatum and right prefrontal cortex in pathological gambling. *Brain Structure and Function*, *220*(1), 469–477.

Krüger, G., & Glover, G. H. (2001). Physiological noise in oxygenation-sensitive magnetic resonance imaging. *Magnetic Resonance in Medicine*, *46*(4), 631–637.

Limbrick-Oldfield, E. H., Van Holst, R. J., & Clark, L. (2013). Fronto-striatal dysregulation in drug addiction and pathological gambling: Consistent inconsistencies? *NeuroImage: Clinical*, *2*, 385–393.

Mohammadi, B., Hammer, A., Miedl, S. F., Wiswede, D., Marco-Pallarés, J., Herrmann, M., & Münte, T. F. (2016). Intertemporal choice behavior is constrained by brain structure in healthy participants and pathological gamblers. *Brain Structure and Function*, *221*(6), 3157–3170.

Piray, P., Den Ouden, H. E., Van Der Schaaf, M. E., Toni, I., & Cools, R. (2015). Dopaminergic modulation of the functional ventrodorsal architecture of the human striatum. *Cerebral Cortex*, 485–495.

Poser, B. A., Versluis, M. J., Hoogduin, J. M., & Norris, D. G. (2006). BOLD contrast sensitivity enhancement and artifact reduction with multi-echo EPI: Parallel-acquired inhomogeneity-desensitized fMRI. *Magnetic Resonance in Medicine*, *55*(6), 1227–1235.

Potenza, M. N., Balodis, I. M., Derevensky, J., Grant, J. E., Petry, N. M., Verdejo-Garcia, A., & Yip, S. W. (2019). Gambling disorder. *Nature Reviews Disease Primers*, *5*(1), 51.

Roeper, J. (2013). Dissecting the diversity of midbrain dopamine neurons. *Trends in Neurosciences*, *36*(6), 336–342.

Rosenbloom, M., & Pfefferbaum, A. (2003). Using magnetic resonance imaging and diffusion tensor imaging to assess brain damage in alcoholics. *Alcohol Research & Health*, *27*(2), 146–152.

Sescousse, G., Janssen, L. K., Hashemi, M. M., Timmer, M. H. M., Geurts, D. E. M., Ter Huurne, N. P., Clark, L., & Cools, R. (2016). Amplified striatal responses to near-miss outcomes in pathological gamblers. *Neuropsychopharmacology*, *41*(10), 2614–2623.

Van Der Schaaf, M. E., Van Schouwenburg, M. R., Geurts, D. E., Schellekens, A. F., Buitelaar, J. K., Verkes, R. J., & Cools, R. (2014). Establishing the dopamine dependency of human striatal signals during reward and punishment reversal learning. *Cerebral Cortex*, *24*(3), 633–642.

Van Holst, R. J., & Boger, M. (2024). Connectivity of the striatum in gambling disorder [Publisher: OSF].

Van Holst, R. J., De Ruiter, M. B., Van Den Brink, W., Veltman, D. J., & Goudriaan, A. E. (2012). A voxel-based morphometry study comparing problem gamblers, alcohol abusers, and healthy controls. *Drug and Alcohol Dependence*, *124*(1), 142–148.

Van Holst, R. J., Veltman, D. J., Büchel, C., Van Den Brink, W., & Goudriaan, A. E. (2012). Distorted expectancy coding in problem gambling: Is the addictive in the anticipation? *Biological Psychiatry*, *71*(8), 741–748.

Van Timmeren, T., Jansen, J. M., Caan, M. W. A., Goudriaan, A. E., & Van Holst, R. J. (2017). White matter integrity between left basal ganglia and left prefrontal cortex is compromised in gambling disorder. *Addiction Biology*, *22*(6), 1590–1600.

Van Timmeren, T., Van Holst, R. J., & Goudriaan, A. E. (2023). Striatal ups or downs? Neural correlates of monetary reward anticipation, cue reactivity and their interaction in alcohol use disorder and gambling disorder. *Journal of Behavioral Addictions*, *12*(2), 571–583.

Van Timmeren, T., Zhutovsky, P., Van Holst, R. J., & Goudriaan, A. E. (2018). Connectivity networks in gambling disorder: a resting-state fMRI study. *International Gambling Studies*, *18*(2), 242–258.

Worhunsky, P. D., Malison, R. T., Rogers, R. D., & Potenza, M. N. (2014). Altered neural correlates of reward and loss processing during simulated slot-machine fMRI in pathological gambling and cocaine dependence. *Drug and Alcohol Dependence*, *145*, 77–86.

Yip, S. W., Morie, K. P., Xu, J., Constable, R. T., Malison, R. T., Carroll, K. M., & Potenza, M. N. (2017). Shared microstructural features of behavioral and substance addictions revealed in areas of crossing fibers. *Biological Psychiatry: Cognitive Neuroscience and Neuroimaging*, *2*(2), 188–195.

Zack, M., St. George, R., & Clark, L. (2020). Dopaminergic signaling of uncertainty and the aetiology of gambling addiction. *Progress in Neuro-Psychopharmacology and Biological Psychiatry*, *99*, 109853.

Zeidman, P., Jafarian, A., Corbin, N., Seghier, M. L., Razi, A., Price, C. J., & Friston, K. J. (2019). A guide to group effective connectivity analysis, part 1: First level analysis with DCM for fMRI. *NeuroImage*, *200*, 174–190.

Zeidman, P., Jafarian, A., Seghier, M. L., Litvak, V., Cagnan, H., Price, C. J., & Friston, K. J. (2019). A guide to group effective connectivity analysis, part 2: Second level analysis with PEB. *NeuroImage*, *200*, 12–25.

Zois, E., Kiefer, F., Lemenager, T., Vollstädt-Klein, S., Mann, K., & Fauth-Bühler, M. (2017). Frontal cortex gray matter volume alterations in pathological gambling occur independently from substance use disorder. *Addiction Biology*, *22*(3), 864–872.